Deoxynivalenol induces caspase-8-mediated apoptosis through the mitochondrial pathway in hippocampal nerve cells of piglet

Jinjie Wu (wjj@ahau.edu.cn)
Anhui Agricultural University https://orcid.org/0000-0001-9706-0808
Xichun Wang
Anhui Agricultural University
Yunjing Jiang
Anhui Agricultural University
Lei Zhu
Anhui Agricultural University
Li Cao
Anhui Agricultural University
Wei Xu
Anhui Agricultural University
Xiaoyan Chu
Anhui Agricultural University
Yafei Zhang
Anhui Agricultural University
Sajid Ur Rahman
Anhui Agricultural University
Shibin Feng
Anhui Agricultural University
Yu Li
Anhui Agricultural University

Research article

Keywords: Deoxynivalenol, apoptosis, mitochondrial pathway, piglet hippocampal nerve cells

Posted Date: October 23rd, 2019

DOI: https://doi.org/10.21203/rs.2.16325/v1

Abstract

Background: Deoxynivalenol (DON) is a common trichothecene mycotoxin found throughout the world. DON has broad toxicity in animals and humans. Its neurotoxicity in vitro, however, is still unclear. This study was designed to investigate the hypothesis that DON toxicity in neurons occurs via the mitochondrial apoptotic pathway.

Results: Using piglet hippocampal nerve cells (PHNCs), we evaluated the effects of varying concentrations of DON on typical indicators of apoptosis. The results obtained demonstrated that DON treatment inhibited PHNC proliferation and led to morphological, biochemical, and transcriptional changes consistent with apoptosis, including decreased mitochondrial membrane potential, mitochondrial release of CYCS and AIF, and increased abundance of active cleaved-caspase-9 and cleaved-caspase-3. Increasing concentrations of DON led to decreased Bcl-2 expression and increased expression of Bax and Bid, which in turn increased transcriptional activity of the transcription factors AIF and P53. Addition of a caspase-8 inhibitor abrogated these effects.

Conclusion: These data reveal that DON induces apoptosis in PHNCs via the mitochondrial apoptosis pathway, and that caspase-8 plays an important role during apoptosis regulation.

Background

Deoxynivalenol (DON) is a mycotoxin named (trichothecene) mostly formed by *F. graminearum* and *F. culmorum,* and is the most common toxin in numerous foods and agricultural products, such as corn, maize, wheat, barley, and oats [1,2]. In many countries, DON pollution in food and feed has been a universal problem, potentially causing poisoning and doing great harm to humans and animals [3–5]. DON has an extensive variety of toxicity in different species. Transformations in pharmacokinetic properties such as, metabolism, absorption, spreading, and removal of DON amongst animal and human species might account for this variance sensitivity. In animal models, the utmost communal consequences of extended nutritional acquaintance to DON are reduced weight gain, anorexia, and malnutrition, with differential susceptibilities observed among different species. *Fusarium* toxin pollution rates and levels are the highest among cereals. DON contamination often occurs with other mycotoxins, although its toxic effects pose the greatest risk to human health and is therefore of significant importance to veterinary medicine, plant breeding, pathology, and public health.

DON toxicity shows dosage and occurrence dependence both in humans and animals, and can cause a range of toxicities including neurotoxicity, cytotoxicity, immunotoxicity, carcinogenesis, and teratogenicity [6–8]. Two well-known neurologic consequences of DON have yielded interest in its neuropharmacologic properties. DON causes anorexia at low dietary concentrations, and induces vomiting at higher doses [9]. DON impairment of weight gain is strongly associated with reduced food intake, which may occur through interference with the motility of intestine and eating desire. These effects likely derive from dysregulation of neuroendocrine signaling within the enteric and central nervous systems [10]. Emesis

associated with DON is thought to be related to its effect on serotonergic signaling. In addition, studies have shown that, DON affects the central nervous system, including effects on neuroendocrine signaling and growth hormone signaling [11].

Recently different studies revealed that DON has extensive toxic effects [12, 13]. However, there remains limited awareness of the neurotoxic effects of DON. The present study focuses on DON-associated neurotoxicity in pig, including its role in cellular apoptosis. Pig is considered to be the most sensitive species to the toxicity of DON [14]. Therefore, we used piglet hippocampal nerve cells (PHNCs) as a neuronal cell model, focusing on mechanisms of DON-induced apoptosis and mitochondrial signaling.

Results

DON induces apoptotic nuclear changes in PHNCs

Laser confocal microscopy was used to detect nuclear features (Fig. 1). Untreated (control) PHNCs showed uniformly blue nuclei (Fig. 1A). However, different concentrations of DON induced significant nuclear changes. The nuclei of DON-treated PHNCs appeared bright blue, and the intensity and proportion of nuclei appearing bright blue increased as DON concentrations increased (Fig. 2B-F).

DON significantly increases rate of apoptosis in PHNCs

Cell apoptosis was investigated by flow cytometry after 24 h of exposure to differing DON concentrations (0, 125, 250, 500, 1000, or 2000 ng/mL). The proportion of cell apoptosis for each of these concentrations of DON is revealed in Fig. 2. Compared to untreated (control) PHNCs, the apoptotic rates for PHNCs in DON treatment groups were increased significantly ($P < 0.01$). The apoptotic rate increased in a dose-dependent way with DON concentrations between 125–1000 ng/mL, while the apoptotic rate of the 2000 ng/mL DON treatment group was lower than that observed for 1000 ng/mL DON. Therefore, 1000 ng/mL of DON was used as the optimal concentration in subsequent trials for addition of caspase–8 inhibitor (FMK).

The influence of DON on feasibility of PHNCs after 24 h incubation was examined via CCK–8 cell viability assay kit. Results showed a dose-dependent decrease in cell viability at DON concentrations from 0–2000 ng/mL range (Fig. 2C). During comparison with the untreated (control) group, the viability of DON-treated cells was significantly decreased ($P < 0.01$), with minimal viability observed for cells medicate with 2000 ng/mL of DON.

DON reduces MMP

MMP was evaluated using flow cytometry after 24 h of DON exposure with different concentrations i-e (0, 125, 250, 500, 1000, or 2000 ng/mL; FMK; 1000 ng/mL + FMK). As shown in Fig. 3, the MMP of DON-treated PHNCs decreased significantly with increasing concentrations of DON, compared to untreated

(control) cells ($P < 0.01$). The MMP was significantly increased in the 1000 ng/mL DON + FMK treatment group compared to the 1000 ng/mL unaided DON treatment group ($P < 0.01$).

Influence of DON on genes expression associated with apoptosis

After PHNCs were bare to specified concentrations of DON (0, 125, 250, 500, 1000, or 2000 ng/mL), FMK, or 1000 ng/mL DON+FMK for 24 h, real-time PCR was used to detect mRNA expression levelsof *Bcl–2, Bax,* and *Bid* (Fig. 4). Compared with untreated (control) PHNCs, the *Bax* and *Bid* mRNA expression levels, as well as the ratio of *Bax/Bcl–2,* were increased significantly ($P<0.01$) with increasing concentrations of DON, topping at a concentration of 1000 ng/mL. The mRNA expression levels of *Bcl–2* and *P53* reduced with increasing concentrations of DON, and when the concentration reached more than 500 ng/mL the expression levels were obviously reduced ($P < 0.01$). In addition, *Bax* and *Bid* mRNA expression levels as well as the *Bax/Bcl*–2 proportion were ominously reduced ($P < 0.01$) in PHNKs treated with 1000 ng/mL DON + FMK compared to treatment with 1000 ng/mL DON alone. *Bcl–2* and *P53* mRNA expression were significantly higher in PHNKs in regard with 1000 ng/mL DON + FMK ($P < 0.01$).

Effects of DON on proteins related with apoptosis

The relative expression of CYCS, AIF, caspase–3, caspase–9, cleaved-caspase–9, and cleaved-caspase3 (Fig. 5A) in DON-treated PHNCs compared to untreated PHNCs shown that, expression of mitochondrial AIF and CYCS (Mito AIF and Mito CYCS) was significantly decreased ($P < 0.01$) with DON concentrations between 250–1000 ng/mL, reaching a minimum at 1000 ng/mL (Fig. 5B). In contrast, expression of AIF and CYCS in the cytoplasm (Cyto AIF and Cyto CYCS) was significantly increased and reached an extreme level at 1000 ng/mL DON.

Cleaved-caspase–9 and cleaved-caspase–3 levels were significantly increased ($P < 0.05$) with DON concentrations between 250–1000 ng/mL, peaking at 1000 ng/mL (Fig. 5B). Caspase–9 and caspase–3 expression was decreased ($P < 0.05$) with DON concentrations between 250–2000 ng/mL. Compared to PHNCs cured with just 1000 ng/mL DON, Mito AIF and Mito CYCS expression in PHNCs treated with 1000 ng/mL DON + FMK was increased but the change was not statistically significant. However, expression of Cyto AIF and Cyto CYCS in PHNCs cured with 1000 ng/mL DON + FMK was significantly decreased ($P < 0.01$). Expression of cleaved-caspase–9 and cleaved-caspase–3 in PHNCs treated with 1000 ng/mL DON + FMK significantly increased ($P < 0.01$), while expression of caspase–9 and caspase–3 in PHNCs treated with 1000 ng/mL DON + FMK showed the opposite effect.

Effect of DON on caspase–3 activity

After 24 h exposure to ascending concentrations of DON (0, 125, 250, 500, 1000, 2000 ng/mL), FMK, or 1000 ng/mL DON + FMK, we found that untreated (control) PHNKs showed minimal or absent expression of caspase–3, while cells cured with DON indicated increasing expression of caspase–3 with higher

concentrations of DON, reached maximum at 1000 ng/mL DON (Fig. 6). Caspase–3 expression was significantly reduced in PHNK cells cured with 1000 ng/mL DON + FMK, after comparison with 1000 ng/mL DON alone.

Effect of DON on the transcriptional activities of AIF and P53

We examined the relationship between mitochondrial release of the transcription factors AIF and P53 and nuclear transcription using EMSA. Transcriptional activities of AIF and P53 in PHNKs treated with DON significantly increased with higher DON concentrations ($P < 0.01$) (Fig. 7). AIF and P53 transcriptional activity was significantly reduced in PHNKs treatment with 1000 ng/mL DON + FMK, when compared to 1000 ng/mL DON alone ($P < 0.01$).

Discussion

DON-induced apoptosis has been confirmed in various cell types including gastrointestinal tract and intestinal epithelial cells. However, there has been no data available on the effects of DON in nerve cells, especially related to DON-induced apoptosis through the mitochondrial signaling pathway. Here we used PHNCs to evaluate this question (schematic, Fig. 8).

DON is known to be toxic to many cell types, with its significant cytotoxicity mediated primarily through induction of apoptosis [15]. The inference of apoptotic chromatin deviates with treatment of DON has been observed by fluorescence microscopy in lung fibroblasts, human proximal tubule cells, and human colon cancer cells [16, 17]. Our experimental results are consistent with these observations. We demonstrated that PHNC viability decreased with increasing concentrations of DON, and that DON-treated cells showed typical ultrastructural changes consistent with apoptosis including nuclear shrinkage and dense fluorescence. These findings collectively propose that DON induces cell death in PHNCs via mitochondrial apoptosis pathway.

DON can damage cell membranes, inhibit cell activity, and promote LDH release, which lead to apoptosis and cell death in PC12 cells [18]. Different concentrations of DON will cause injury to cells in varying degrees. Many studies have shown that DON can inhibit cell proliferation in a dose-dependent manner [19, 20]. Even low concentrations of DON may cause apoptosis, with increasing rates of apoptosis as DON concentrations increase. At higher concentrations DON mostly caused cell death and also may cause a little apoptosis [21]. We confirmed using flow cytometry that apoptosis occurs in a DON dose-dependent fashion in PHNCs; we observed a higher rate of apoptosis in cells cured with 1000 ng/mL of DON compared to 2000 ng/mL DON, but higher cell death at 2000 ng/mL DON compared to 1000 ng/mL DON. These results are consistent with earlier observations. Overall, the above results revealed that DON can persuade apoptosis of PHNCs, suggesting that further research focusing on the mitochondrial apoptotic pathway is warranted.

Caspase–8 is known to play a crucial role in intervening Fas-persuaded apoptosis [22, 23]. In this paradigm, Fas ligand- or agonistic antibody-mediated cross-linkage of the Fas receptor that leads to assembly of the death inducing signal complex (DISC), of which the adaptor FADD/MORT–1 and caspase–8 form a part [24].Association of this complex leads to initiation of caspase–8, which pledges the classic apoptotic cascade including activation of caspase–3, –6, and –7, and ultimately mitochondrial damage [25]. During apoptosis which are activated by Fas, a subcategory of caspase family associates is triggered. Among them is caspase–8, which activates additional downstream caspases and directs the cell toward apoptosis. In light of its central role in apoptosis, we chose an inhibitor of caspase–8 to demonstrate the role of the mitochondrial apoptosis pathway in DON-associated toxicity.

Mitochondria are one of the most important cellular organelles for cellular energy production and survival, and the mitochondrial pathway is the utmost vital intracellular apoptosis signaling cascade. The mitochondrial membrane potential (MMP) results from the uneven distribution of protons and ions across the mitochondrial membrane. Recently researchers have also shown that variations in MMP and mitochondrial permeability play a significant role in the process of apoptosis, and it is thought that alterations in MMP occur in the earliest stages of apoptosis. Once mitochondria are injured, the MMP is markedly decreased, leading to severe impairment of mitochondrial function and eventually irreversible apoptosis. In recent years, studies have shown that mitochondria are involved in almost all cell apoptosis [26]. In this study, we labeled mitochondria of apoptotic cells with JC–1 and measured fluorescence using flow cytometry to quantify changes in MMP. We found that MMP of PHNCs decreased significantly after 24 h exposure to concentrations of DON in ascending order. MMP was significantly increased in PHNCs cured with 1000 ng/mL DON + FMK compared to 1000 ng/mL alone ($P < 0.01$), suggesting that caspase–8 inhibition can prevent dissipation of the MMP. Altogether, these data confirmed that mitochondria are involved in DON-mediated cell apoptosis.

For the first time B-cell lymphoma/leukemia–2 (Bcl–2) was known in a study of B-cell lymphoma, and overexpression of Bcl–2 protein can inhibit apoptosis and prolong cell life. Bcl–2 was the first protein to be recognized as an inhibitor of apoptosis. Bcl–2 protein is contained on the endoplasmic reticulum, mitochondrial membrane, and the nuclear envelope, through a region in its C-terminus [27–29].

Bcl–2 has been shown to be the most important protein that inhibits tumor cell apoptosis. There are more than 25 members of Bcl–2 family have been identified. Studies propose that that Bcl–2 may act on signaling molecules and mitochondrial and nuclear pore complexes such as CYCS and apoptosis inducing factor AIF, and control cell signaling to prolong cell survival [30]. The Bcl–2/Apaf–1/caspase–9 complex is directly combined with Apaf–1 to inhibit the activation of caspase–9 by caspase–3. Bcl–2 may also regulate caspase on the mitochondrial membrane and reduce its activity, but it does not affect the activation of caspase–9 by CYCS and Apaf–1 [31]. Bcl–2 protein can inhibit apoptosis by binding to Bid, Bim, or Bad, and Bcl–2/Bax ratio concludes whether a cell will live after receiving apoptotic signals [32].

Bid is a pro-apoptotic factor and its product, tBid, has the ability to induce CYCS leakage from mitochondria [33–35], without dissipation of the mitochondrial inner membrane potential. Bid does not possess activity under normal physiological conditions. With the initiation of apoptosis, caspase–8 is activated first, and then the Bid enzyme is cleaved into dual number of fragments, namely a C-terminal fragment and an N-terminal fragment of 15 kD. C-fragments are transferred from the cytoplasm to mitochondria and induce release of CYCS from mitochondria, while N- fragments remain in the cytoplasm and cannot induce the release of CYCS. In our study, *bcl–2* expression declined with higher concentration of DON, with expression reaching a lowest at 1000 ng/mL. However, changes in *bax* expression showed an opposite trend, as found by earlier observations [36, 37]. With increasing of DON concentration, *bid* expression also increased, and at 1000 ng/mL it reached a maximum level. We suspect that the increase in expression of *bid* at the transcriptional level reflectsincreased levels of active Bid. Variations in expression of *bcl–2, bax* and *bid* in PHNCs preserved with 1000 ng/mL DON + FMK were contrary to those cured with 1000 ng/mL DON alone. Our data support the conclusion that *bcl–2, bax,* and *bid* act a decisive role in apoptosis in DON-treated cells.

A water-soluble mitochondrial inner membrane protein called Cytochrome C that plays a fundamental role in the transportation of electron in the respiratory chain. CYCS released from the mitochondria into the cytoplasm after stimulation by an apoptotic signal, further increasing caspase–3 and caspase–9 activation [38]. We found that mitochondrial CYCS abundance decreased as DON concentration increased, with the greatest effect observed at at 1000 ng/mL DON. Nevertheless, mitochondrial levels of CYCS in PHNCs treated with 1000 ng/mL DON + FMK were higher than in cells cured with 1000 ng/mL DON alone. These data propose that CYCS is unconstrained into the cytoplasm from mitochondria when DON-triggered apoptosis occurred, and that caspase–8 inhibition via FMK could prevent the release of CYCS from the mitochondria.

AIF is an active protein of induced apoptosis, located between the mitochondrial double membranes. AIF is free from the mitochondria into the cytoplasm after stimulation by an apoptosis signal, enters nucleus where it facilitates DNA cleavage, which may further contribute to apoptosis [39]. In our previous study [18], we found that AIF was released into the cytoplasm from the mitochondria in cells treated with DON, and that this release was prohibited by FMK-mediated inhibition of caspase–8.

Caspases are a family of cysteine proteases that can specifically shear peptide bonds that follow aspartic acid residues, and have the capacity for autocatalysis and mutual activation [40]. Caspase proteases play a vital role in signal transduction during cell apoptosis, and cleaved caspases hydrolyze important proteins involved in cell regulation, cell signal transduction, and DNA restoration [41]. Caspase–3 is located downstream of the initial triggers of cell apoptosis; cleaved caspase–3 acts directly on the nucleus and mediates apoptosis. Apoptosis signal in the cell could induce the formation of a PT (permeability transition) channel and endorse the discharge of CYCS from the mitochondria. CYCS, Apaf–1, ATP, or ADP and caspase–9 zymogen form an apoptosis-promoting complex, from which caspase–9 is released and activated [42]. Triggered caspase–9 cleaves downstream caspase–3 zymogen, leading to its activation, while caspase–3 degrades substrates lead to rupture of the nuclear

fiber lamina and compaction of nuclear chromatin, resulting in cell apoptosis [43]. In the present experiment, DON treatment significantly augmented the expression of cleaved-caspase–9 and cleaved-caspase–3 in PHNCs, and decreased the relative expression of caspase–9 and caspase–3 compared to untreated (control) cells. The abundance of cleaved-caspase–9 and cleaved-caspase–3 in PHNCs cured with 1000 ng/mL DON + FMK was lesser than that in cells canned with 1000 ng/mL DON. The expression of caspase–9 and caspase–3 in cells treated with 1000 ng/mL DON + FMK showed the opposite trends. These results indicated that CYCS, AIF, caspase–9, and caspase–3 contribute in DON-triggered apoptosis in PHNCs.

The tumor suppressor gene P53, a transcription factor central to regulation of apoptosis, possesses two functions: to repair cell damage or to induce cell apoptosis. P53 could combine with DNA and checked if DNA was damaged. After DNA damage was founded by P53, it would stimulate the expression of CIP (CDK-interacting protein), preventing cell division and allowing for DNA repair to occur. When DNA damage was higher than P53 repair, then the expression of P53 could promote cell apoptosis [44, 45]. P53 could affect cell apoptosis through inhibiting the *Bcl–2* expression level and endorsing *Bax* and *Bak* expression [46].In our study, the transcription activities of P53 were enhanced with the increasing DON concentration, which confirmed the effect of P53 in cell apoptosis.

In summary, the present study indicates that DON can induce apoptosis of PHNCs via triggering of mitochondrial signal transduction pathway. Our study found that DON treatment led to induction of the pro-apoptotic genes *Bax* and *Bid,* while *Bcl–2* expression was repressed. DON treatment also led to cleavage (activation) of the apoptosis-related proteins caspase–3 and caspase–9. These effects were diminished by inhibition of caspase–8. Together, these data propose that mitochondrial apoptosis might be a principal mechanism through which DON persuades neurotoxicity, and provide important insights for future studies on mechanisms of DON neurotoxicity.

Materials And Methods

Cell culture and treatment

The Piglet hippocampal nerve cells (PHNCs) were provided by Nanjing Keygen Biological Technology which were cultured in Dulbecco's Modified Eagle Medium (DMEM) (Thermo Scientific, Grand Island, NY) comprising of Fetal Bovine Serum (FBS, 10%), (Clark Bioscience, Richmond, VA), and 100 U/mL of penicillin, with 100 μg/ml streptomycin under an atmosphere of 5% CO_2. For ultrastructural studies and apoptosis assays, PHNCs were grow in logarithmic phase, harvested and seeded in 24-well plates (110^5 cells/mL). The cells were incubated for 24 h and cured with ascending concentrations of DON (Sigma, St. Louis, MO) (0, 125, 250, 500, 1000, 2000 ng/mL) for 24 h. In two experimental groups, caspase–8 inhibitor (FMK, Keygen Biotech, Nanjing, China) was added (0, 1000 ng/mL DON) 30 minutes prior to DON treatment to assess the mitochondrial caspase–8-mediated apoptosis pathway in DON exposure response. Cells were collected for evaluation of Cytochrome C, AIF, caspases, and *bcl–2* family members.

Viability assay

CCK–8 cell viability assay kit (Dojindo Molecular Technologies, Inc., Tokyo, Japan) was used to detect cell viability rendering to the protocol of manufacturer's. Briefly, 110^5 cells/mL in a volume of 100 µL DMEM in 96-well plates were hatched for 24 h and then cured with DON for 24 h. After 3 h incubation with 10 µL CCK–8 reagent each well, absorption at 450 nm were determined on a plate photometer (Thermo Scientific, Waltham, MA).

Hoechst 33258 staining

The impact of DON on the nuclear chromatin of cells was observed by Hoechst 33258 staining. On sterile cover glasses PHNCs were seeded and placed in 24-well plates for 24 h. The cells were then treated with the indicated concentrations of DON (0, 125, 250, 500, 1000, 2000 ng/mL) for 24 h. Cold PBS buffer were used to washed cells and fixed with 4% formaldehyde for 30 min, and then hatched with 100 µL Hoechst 33258 staining solution for 5 min. After washing three times with PBS, the cells were viewed under a FV1000 Laser confocal microscope (Olympus, Japan).

Determination of apoptotic cells

An Annexin V-FITC/PI Cell apoptosis assay kit (Wanleibio, Shenyang, China) was used to measure cell apoptosis. After treating for 24 h with different concentrations of DON, the cells were collected using two PBS washes. 500 µL obligatory buffers were added to re-suspend the cell pellet, with the adding of 5 µL annexin V-binding and 5 µL propidium iodide (PI). Cells were stained for 15 min in the dark at room temperature, and then examined for apoptosis by a method called flow cytometry using 10,000 cells per sample (Becton Dickinson, Franklin Lakes, NJ, USA).

Detection of the mitochondrial membrane potential (MMP)

JC–1 Fluorescence Kit (Thermo Scientific) was used to measure mitochondrial membrane potential (MMP). PHNCs were treated with different concentrations of DON, FMK, or 1000 ng/mL DON+FMK for 24 h. JC–1 working solution was prepared in the proportion of 500 µL 1× Incubation Buffer to 1 µL JC–1. Cell pellets were re-suspended in 500 µL JC–1 operational solution and the cells were hatched for 15 min at 37°C. The collected cells were washed two times with 500 µL 1× Incubation Buffer. Cells were then re-suspended in 500 µL 1× Incubation Buffer and evaluated by flow cytometry.

RT-PCR analysis

In PHNCs expression of Bcl–2 family members was detected by RT-PCR. The cells were cured with DON in different concentrations, FMK, and 1000 ng/mL DON + FMK for 24 h, respectively. Total RNA was isolated via Trizol (TaKaRa, Dalian, China), and cDNA was synthesized followed by a RT-PCR kit (Takara)

rendering to the protocol of manufacturer's. The designed primers are listed in Table 1. PCR conditions were 95°C for 1 min, followed by 40 cycles of 95°C for 15 s, 58°C for 20 s, and 72°C for 20 s.

Western blot analysis

To determined protein levels of cleaved-caspase–3, cleaved-caspase–9, Cytochrome C, and AIF western blot analysis was used. DON was used in different concentration treat PHNC, FMK, and 1000 ng/mL DON+FMK. A mitochondria/cytosol fractionation kit (Beyotime Inst. Biotech, Beijing, China) was used to isolate mitochondrial and cytosolic proteins. Aliquots of 50 μg proteins were detached on a 12% SDS-polyacrylamide gel for cleaved-caspase–9, cleaved-caspase–3 and AIF, and on a 15% gel for cytochrome C, and then moved to PVDF membrane. Membranes were blocked with TBST buffer containing 5% bovine serum albumin and incubated with antibodies against β-actin (1:7500), AIF (1:200), CYCS (1:200), cleaved-caspase–3 (1:750), and cleaved-caspase–9 (1:750) at 4°C overnight, followed by addition of horseradish peroxidase-linked anti-mouse/rabbit IgG. The bands were imagined via Super Signal West femto kit.

Immunofluorescence analysis

The activity of caspase–3 was analyzed by immunocytofluorescence using laser confocal microscopy (FV100, Olympus, Japan). Briefly, PHNCs were grown-up on cover slips and hatched with DON in different concentration, FMK, or 1000 ng/mL DON + FMK for 24 h and washed with cold PBS. After being static with 4% paraformaldehyde and with PBS washed thrice, the cells were permeabilized with 0.02% Triton X–100 for 3 min. Cells were blocked for 30 min at room temperature in 5% BSA, and hatched with cleaved-caspase–3 antibody at 4°C for the whole night with secondary antibody (1:200) for 1 h. It was then washed thrice with PBS; nuclei were stained with DAPI for 3 min. Pictures were taken via Olympus FV10-ASW 1.7 Viewer software (Olympus, Japan).

Transcriptional activity

The transcriptional activities of transcription factor AIF and P53 were determined by electrophoretic mobility shift assay (EMSA). A nuclear protein extraction kit (Sangon Biotech Co., Ltd., Shanghai, China) was used to isolate nuclear proteins. The concentrations of nuclear proteins were determined by Bio-Rad protein assay reagent (Sangon Biotech Co., Ltd., Shanghai, China). The binding reaction of extracted nuclear proteins (6 μg) with biotin-labeled probe was performed rendering to the protocol of manufacturer's. The complexes were detached by electrophoresis on non-denaturating 6% polyacrylamide Tris/borate/EDTA (TBE) gels and moved into a membranes made up of nylon. Membranes were crosslinked by a UV cross-linker (Cany Precision Instruments Co., Ltd., Shanghai, China) and the probe was noticed with the help of enhanced chemiluminescence solution (ECL; Pierce Biotechnology Inc., Chicago, IL, USA).

Statistical analysis

All the data were expressed as mean ± standard deviation (SD). One-way ANOVA were used for statistical comparison, followed by Tukey's *post hoc* test. $P < 0.05$ was measured statistically significant.

Declarations

Abbreviations

CYCS: Cytochrome c; AIF: Apoptosis Inducing Factor; Bcl–2: B-cell lymphoma–2; Bax: Bcl–2-associated X protein; Bid: bh3 interacting domain death agonist PHNCs: piglet hippocampal nerve cells; caspase: cysteineaspartic proteases

FMK: caspase–8 inhibitor; CCK–8: Cell Counting Kit–8; RT-PCR:Reverse Transcription-Polymerase Chain Reaction.

Acknowledgments

The authors deeply acknowledge the collaboration of veterinary graduate students Xiaofang Chen, Yingying Huang, Chenglu Peng.

Author Contribution Statement

X. C. W., Y. J. J., and L.Z wrote the manuscript and participated in the design or implementation of the study. L. C and W. X performed the experiments and analyzed the data. X. Y. C., Y. F. Z., R. S., S. B. F., Y, L., and J. J. W. performed the literature search, data collection, analysis and interpretation, and created the figures. All authors approved the final version of the manuscript.

Funding

The present study was supported by the National Natural Science Foundation of China (grant No. 31472250) and the Project of Modern Agricultural Industry and Technology System of Anhui Province (grant No. AHCYJSTX–05–07). We wish to thank anonymous reviewers for their kind advice.

Availability of data and materials

The datasets used and/or analyzed during the study are available from the corresponding author on reasonable request

Conflicts of interest

The authors declare no competing financial interests.

Author details

College of Animal Science and Technology, Anhui Agricultural University, Hefei 230036, China

References

1. Wegulo SN. Factors Influencing Deoxynivalenol Accumulation in Small Grain Cereals. Toxins. 2012; 4(11):1157-1180.

DOI: 10.3390/toxins4111157

2. Binder EM, Tan LM, Chin LJ, Handl J and Richard J. Worldwide occurrence of mycotoxins in commodities, feeds and feed ingredients. Animal Feed Science & Technology. 137;(3-4):265-282.

DOI: 10.1016/j.anifeedsci.2007.06.005

3. Mudili V, Siddaih CN, Nagesh M, Garapati P, Naveen KK, Murali HS, Yli MT and Batra HV. Mould incidence and mycotoxin contamination in freshly harvested maize kernels originated from India. Journal of the Science of Food & Agriculture. 2014; 94(13):2674.

DOI: 10.1002/jsfa.6608

4. Nordkvist E and Häggblom P. Fusarium mycotoxin contamination of cereals and bedding straw at Swedish pig farms. Animal Feed Science & Technology. 2014; 198:231-237.

DOI: 10.1016/j.anifeedsci.2014.10.002

5. Brera C, Bertazzoni V, Debegnach F, Gregori E, Prantera E and De SB. Exposure assessment for Italian population groups to deoxynivalenol deriving from pasta consumption. Toxins. 2013; 5(12):2293.

DOI: 10.3390/toxins5122293

6. Wang X, Fan M, Chu X, Zhang Y, Rahman SU, Jiang Y, Chen X, Zhu D, Feng S, Li, Y and Wu J. Deoxynivalenol induces toxicity and apoptosis in piglet hippocampal nerve cells via the MAPK signaling pathway. Toxicon. 2018;155: 1-8 .

DOI 10.1016/j.toxicon.2018.09.006

7. Singh S, Banerjee S, Chattopadhyay P, Borthakur SK and Veer V. Deoxynivalenol induces cytotoxicity and genotoxicity in animal primary cell culture. Toxicology Methods. 2015; 25(3):184-191.

DOI: 10.3109/15376516.2015.1006743

8. Wang X, Tang J, Geng F, Zhu L, Chu X, Zhang Y, Rahman SU, Chen X, Jiang Y, Zhu D, Feng S, Li Y and Wu J. Effects of deoxynivalenol exposure on cerebral lipid peroxidation, neurotransmitter and calcium homeostasis of chicks in vivo. Toxicon. 2018;150:60-65.

DOI 10.1016/j.toxicon.2018.05.010

9. Pestka JJ, Lin WS and Miller ER. Emetic activity of the trichothecene 15-acetyldeoxynivalenol in swine. Food & Chemical Toxicology. 1987;25(11):855-858.

DOI: 10.1016/0278-6915(87)90264-X

10. Krantis A and Durst T. Novel multi-ring organic compounds for regulating gut motility and food intake. US, 10/250986, 2002-1-11. 2006.
11. Awad WA, Aschenbach JR, Setyabudi FMCS, Razzazifazeli E, Böhm J and Zentek J. In Vitro Effects of Deoxynivalenol on Small Intestinal d-Glucose Uptake and Absorption of Deoxynivalenol Across the Isolated Jejunal Epithelium of Laying Hens. Poultry Science. 2007;86(1):15-20.

DOI: 10.1093/ps/86.1.15

12. Gaigé S, Bonnet MS, Tardivel C, Pinton P, Trouslard J, Jean A, Guzylack L, Troadec JD and Dallaporta M. c-Fos immunoreactivity in the pig brain following deoxynivalenol intoxication: focus on NUCB2/nesfatin-1 expressing neurons. Neurotoxicology. 2013; 34(1):135-149.

DOI: 10.1016/j.neuro.2012.10.020

13. Gu W, Zhu P, Jiang D, He X, Li Y, Ji J, Zhang L, Sun Y and Sun X. A novel and simple cell-based electrochemical impedance biosensor for evaluating the combined toxicity of DON and ZEN. Biosensors & Bioelectronics. 2015; 70:447-454.

DOI:10.1016/j.bios.2015.03.074

14. Rotter BA, Prelusky DB and Pestka JJ. Toxicology of deoxynivalenol (vomitoxin). Journal of Toxicology & Environmental Health. 1996; 48(1):1-34.

DOI: 10.1080/713851046

15. Mikami O, Yamamoto S, Yamanaka N and Nakajima Y. Porcine hepatocyte apoptosis and reduction of albumin secretion induced by deoxynivalenol. Toxicology. 2004; 204(2):241-249.

DOI: 10.1016/j.tox.2004.07.001

16. Königs M, Lenczyk M, Schwerdt G, Holzinger H, Gekle M and Humpf HU. Cytotoxicity, metabolism and cellular uptake of the mycotoxin deoxynivalenol in human proximal tubule cells and lung fibroblasts in primary culture. Toxicology. 2007;240(1):48-59.

DOI: 10.1016/j.tox.2007.07.016

17. Ma Y, Zhang A, Shi Z, He C, Ding J, Wang X, Ma J and Zhang H. A mitochondria-mediated apoptotic pathway induced by deoxynivalenol in human colon cancer cells. Toxicology in Vitro. 2012;26(3):414.

DOI: 10.1016/j.tiv.2012.01.010

18. Wang X, Xu W, Fan M, Meng T, Chen X, Jiang Y, Zhu D, Hu W, Gong J and Feng S. Deoxynivalenol induces apoptosis in PC12 cells via the mitochondrial pathway. Environmental Toxicology & Pharmacology. 2016; 43:193.

DOI: 10.1016/j.etap.2016.03.016

19. Ji GE, Park SY, Wong SS and Pestka JJ. Modulation of nitric oxide, hydrogen peroxide and cytokine production in a clonal macrophage model by the trichothecene vomitoxin (deoxynivalenol). Toxicology. 1998;125(2-3):203-214.

DOI: 10.1016/S0300-483X(97)00178-9

20. Bensassi F and El GBEES. Pathway of deoxynivalenol-induced apoptosis in human colon carcinoma cells. Toxicology. 2009;264(1):104-109.

DOI: 10.1016/j.tox.2009.07.020

21. Ren Z, Wang Y, Deng H, Deng Y, Deng J, Zuo Z, Wang Y, Peng X, Cui H and Shen L. Deoxynivalenol induces apoptosis in chicken splenic lymphocytes via the reactive oxygen species-mediated mitochondrial pathway. Environmental Toxicology & Pharmacology. 2015;39(1):339-346.

DOI: 10.1016/j.etap.2014.11.028

22. Boldin MP, Goncharov TM, Goltsev YV and Wallach D. Involvement of MACH, a novel MORT1/FADD-interacting protease, in Fas/APO-1- and TNF receptor-induced cell death. Cell . 1996;85(6):803-815.

DOI: 10.1016/S0092-8674(00)81265-9

23. Fernandesalnemri T, Armstrong RC, Krebs J, Srinivasula SM, Wang L, Bullrich F, Fritz LC, Trapani JA, Tomaselli KJ, Litwack, G and Alnemir ES. In vitro activation of CPP32 and Mch3 by Mch4, a novel human apoptotic cysteine protease containing two FADD-like domains. Proceedings of the National Academy of Sciences of the United States of America. 1996;93(15): 7464-7469.

DOI: 10.1073/pnas.93.15.7464

24. Kischkel FC, Hellbardt S, Behrmann I, Germer M, Pawlita M, Krammer PH and Peter ME. Cytotoxicity-dependent APO-1 (Fas/CD95)-associated proteins form a death-inducing signaling complex (DISC)

with the receptor. Embo Journal. 1995;14(22):5579-5588.

PMID: 8521815

25. Salvesen GS and Dixit VM. Caspases: intracellular signaling by proteolysis. Cell. 1997;91(4):443-446.

DOI: 10.1016/S0092-8674(00)80430-4

26. Benzie IFF and Strain JJ. The Ferric Reducing Ability of Plasma (FRAP) as a Measure of “Antioxidant Power”: The FRAP Assay. Analytical Biochemistry. 1996, 239(1):70-76.

DOI: 10.1006/abio.1996.0292

27. Tsujimoto Y, Finger LR, Yunis J, Nowell PC and Croce CM. Cloning of the chromosome breakpoint of neoplastic B cells with the t(14;18) chromosome translocation. Science. 1984;226(4678):1097-1099.
28. Vaux DL, Cory S and Adams JM. Bcl-2 gene promotes haemopoietic cell survival and cooperates with c-myc to immortalize pre-B cells. Nature. 1988;335(6189):440.

DOI: 10.1038/335440a0

29. Reed JC. Bcl-2 and the regulation of programmed cell death. Journal of Cell Biology 1994;124(1):1-6.

PMID: 8294493

30. Sutton VR, Davis JE, Cancilla M, Johnstone RW, Ruefli AA, Sedelies K, Browne KA and Trapani JA. Initiation of apoptosis by granzyme B requires direct cleavage of bid, but not direct granzyme B-mediated caspase activation. Journal of Experimental Medicine. 2000;192(10):1403.

PMID: 11085743

31. Farrow SN, White JH, Martinou I, Raven T, Pun KT, Grinham CJ, Martinou JC and Brown R. Cloning of a bcl-2 homologue by interaction with adenovirus E1B 19K. Nature. 1995;374(6524):731.

DOI: 10.1038/374731a0

32. Krajewski S, Krajewska M, Shabaik A, Miyashita T, Wang HG and Reed JC. Immunohistochemical determination of in vivo distribution of Bax, a dominant inhibitor of Bcl-2. American Journal of Pathology. 1994;145(6):1323-1336.

PMID: 7992838

33. Luo X, Budihardjo I, Zou H, Slaughter C and Wang X. Bid, a Bcl2 Interacting Protein, Mediates Cytochrome c Release from Mitochondria in Response to Activation of Cell Surface Death Receptors. Cell. 1998;94(4):481-490.

DOI: 10.1016/j.tiv.2012.01.010

34. Li H, Zhu H, Xu CJ and Yuan J. Cleavage of BID by caspase 8 mediates the mitochondrial damage in the Fas pathway of apoptosis. Cell. 1998, 94(4):491-501.

DOI: 10.1016/S0092-8674(00)81590-1

35. Cheng EH, Kirsch DG, Clem RJ, Ravi R, Kastan MB, Bedi A, Ueno K and Hardwick JM. Conversion of Bcl-2 to a Bax-like death effector by caspases. Science. 1997;278(5345):1966-1968.

DOI: 10.1126/science.278.5345.1966

36. Lovell JF, Billen LP, Bindner S, Shamas-Din A, Fradin C, Leber B and Andrews DW. Membrane binding by tBid initiates an ordered series of events culminating in membrane permeabilization by Bax. Cell. 2008;135(6):1074-1084.

DOI: 10.1016/j.cell.2008.11.010

37. Youle RJ and Strasser A. The BCL-2 protein family: opposing activities that mediate cell death. Nature Reviews Molecular Cell Biology. 2008;9(1):47-59.

DOI: 10.1038/nrm2308

38. Vogt PK and Reed. Cyclin-Dependent Kinase (CDK) Inhibitors. Methods in Molecular Biology. 2006;1336.

PMID:26722102

39. Lemarié A, Lagadicgossmann D, Morzadec C, Allain N, Fardel O and Vernhet L. Cadmium induces caspase-independent apoptosis in liver Hep3B cells: role for calcium in signaling oxidative stress-related impairment of mitochondria and relocation of endonuclease G and apoptosis-inducing factor. Free Radical Biology & Medicine. 2004;36(12):1517-1531.

DOI: 10.1016/j.freeradbiomed.2004.03.020

40. Jiang X and Wang X. Cytochrome C-mediated apoptosis. Annual Review of Biochemistry. 2004;73(73):87-106.

DOI: 10.1146/annurev.biochem.73.011303.073706

41. Thornberry NA and Lazebnik Y. Caspases: enemies within. Science.1998;281(5381):1312 .

DOI: 10.1126/science.281.5381.1312

42. Budihardjo I, Oliver H, Lutter M, Luo X and Wang X. Biochemical pathways of caspase activation during apoptosis. Annu Rev Cell Dev Biol. 1999;15(1):269-290.

DOI: 10.1146/annurev.cellbio.15.1.269

43. Reed JC. Mechanisms of apoptosis avoidance in cancer. Current Opinion in Oncology. 1999;11(1):68-75.

DOI: 10.1097/00001622-199901000-00014

44. Miyashita T and Reed JC. Tumor suppressor p53 is a direct transcriptional activator of the human bax gene. Cell. 1995;80(2):293-299.

DOI: 10.1016/0092-8674(95)90412-3

45. Clarke AR, Gledhill S, Hooper ML, Bird CC and Wyllie AH. p53 dependence of early apoptotic and proliferative responses within the mouse intestinal epithelium following gamma-irradiation. Oncogene. 1994;9(6):1767-1773..

PMID: 8183575

46. Johnstone RW, Ruefli AA and Lowe SW. Apoptosis: a link between cancer genetics and chemotherapy. Cell. 2002;108(2):153-164.

DOI: 10.1016/S0092-8674(02)00625-6

Table 1

Table 1. Parameters of primer for *Bcl-2, Bax, Bid, P53*and *GAPDH* genes

Gene	Accession number	Primer	Sequences (5′→3′)	Product/bp
GAPDH	NM_002046	Forward	GGTGAAGGTCGGTGTGAACG	232
		Reverse	CTCGCTCCTGGAAGATGGTG	
Bcl-2	NC_000067.6	Forward	TGGGATGCCTTTGTGGAACT	153
		Reverse	GCAGGTTTGTCGACCTCACT	
Bax	NC_000073.6	Forward	GGTTTCATCCAGGATCGAGCA	151
		Reverse	TCCTCTGCAGCTCCATATTGC	
Bid	NM_197966.1	Forward	AGCTACACAGCTTGTGCCAT	186
		Reverse	CAGCTCGTCTTCGAGGTCTG	
P53	NC_000077.6	Forward	CCCAAACTGCTAGCTCCCAT	217
		Reverse	GGAGGATTGTGTCTCAGCCC	

Figures

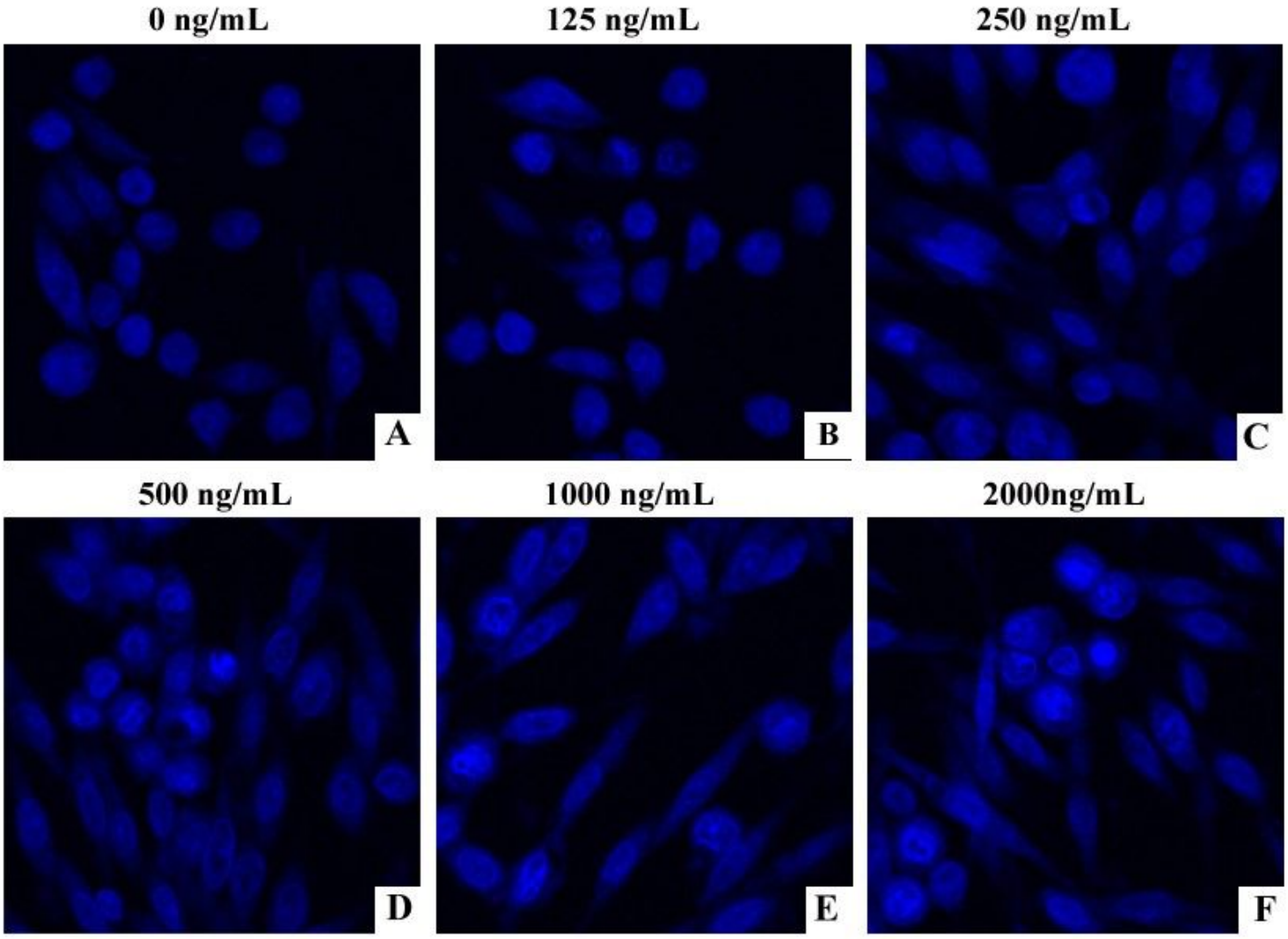

Figure 1

Apoptotic nuclear morphological changes highlighted by Hoechst 33258 staining in cells treated with graded concentration of DON (0-2000 ng /mL) for 24 h.

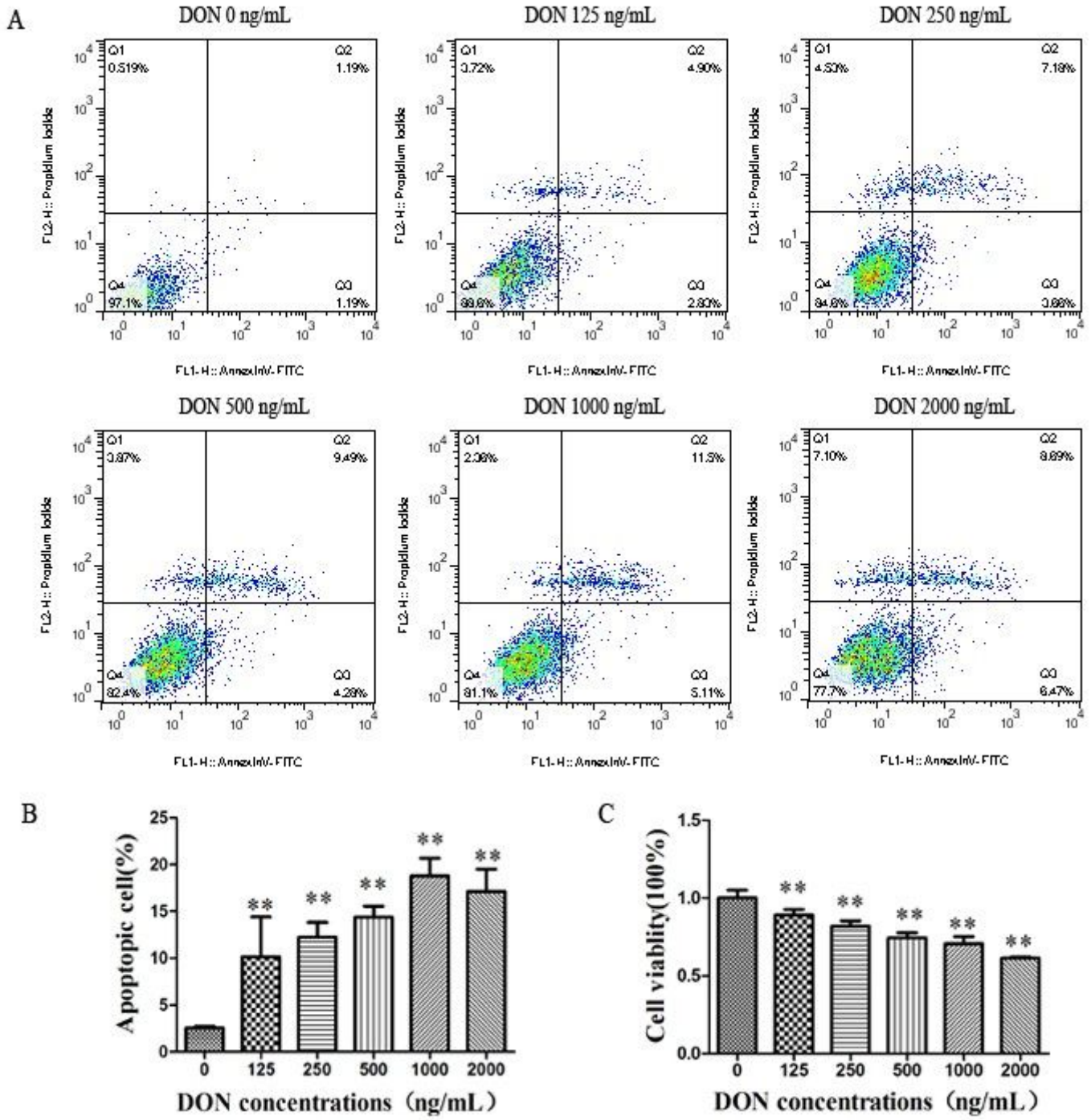

Figure 2

Effect of DON on PHNCs apoptosis rate and cells activity. A. Different concentration of DON-treated PHNCs apoptosis picture. B. The effect of different concentration of DON on PHNCs apoptosis rate. C. The effect of different concentration of DON on PHNCs activity .Date are mean values ± SD (n = 3). **Highly significant difference vs. controls (P< 0.01).

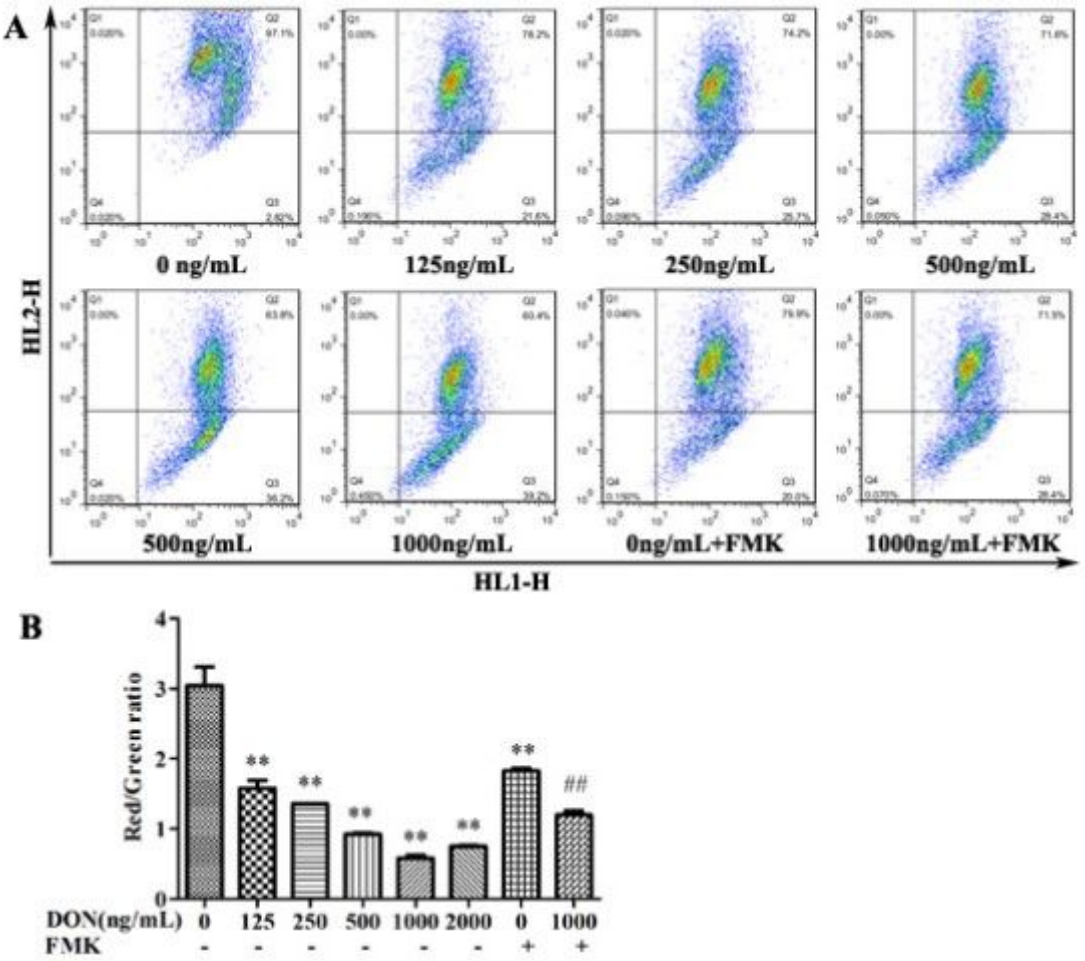

Figure 3

Effect of DON on mitochondrial membrane potentials in PHNCs. A. Different concentration of DON-treated PHNCs mitochondrial membrane potentials picture. B. The effect of different concentration of DON on PHNCs mitochondrial membrane potentials. Date are mean values ± SD (n = 3). ** Highly significant difference vs. controls ($P < 0.01$). ## Highly significant difference vs. 1000 ng/mL DON group ($P < 0.01$).

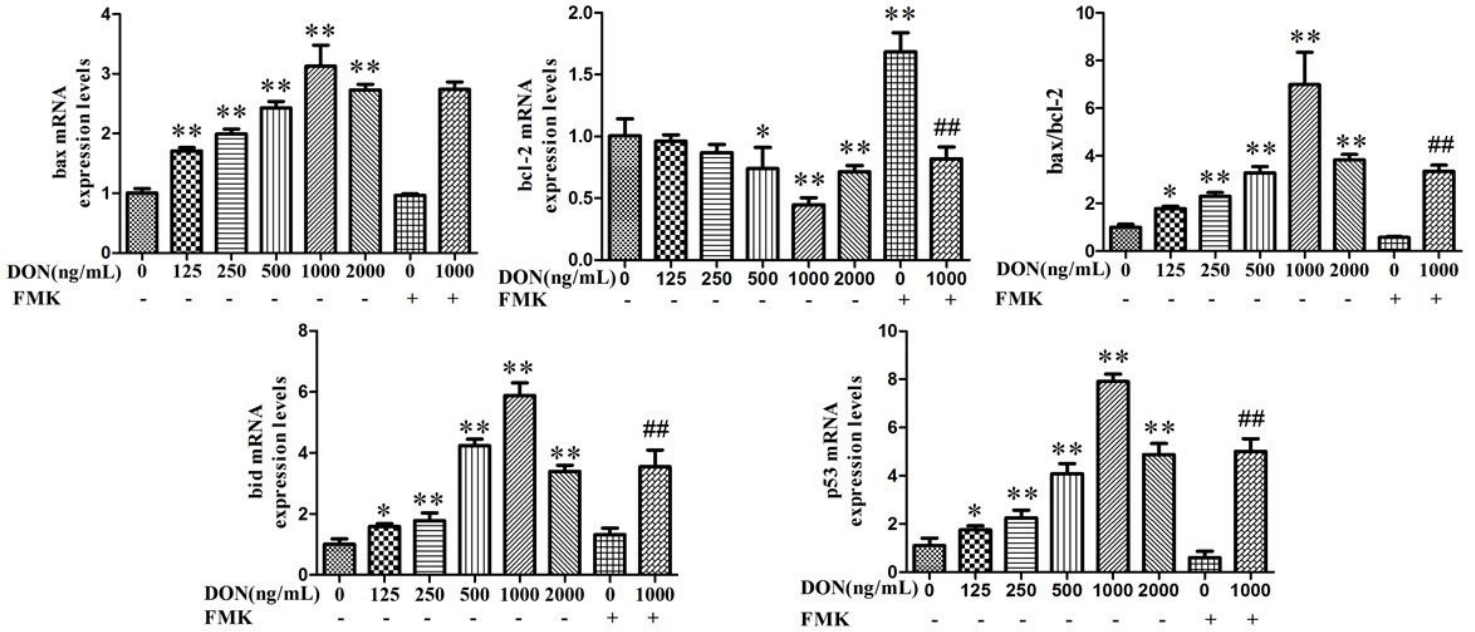

Figure 4

Effect of DON on apoptosis-related gene expression. Date are mean values ± SD (n = 3). ** Highly significant difference vs. controls (P < 0.01). ## Highly significant difference vs. 1000 ng/mL DON group (P < 0.01).

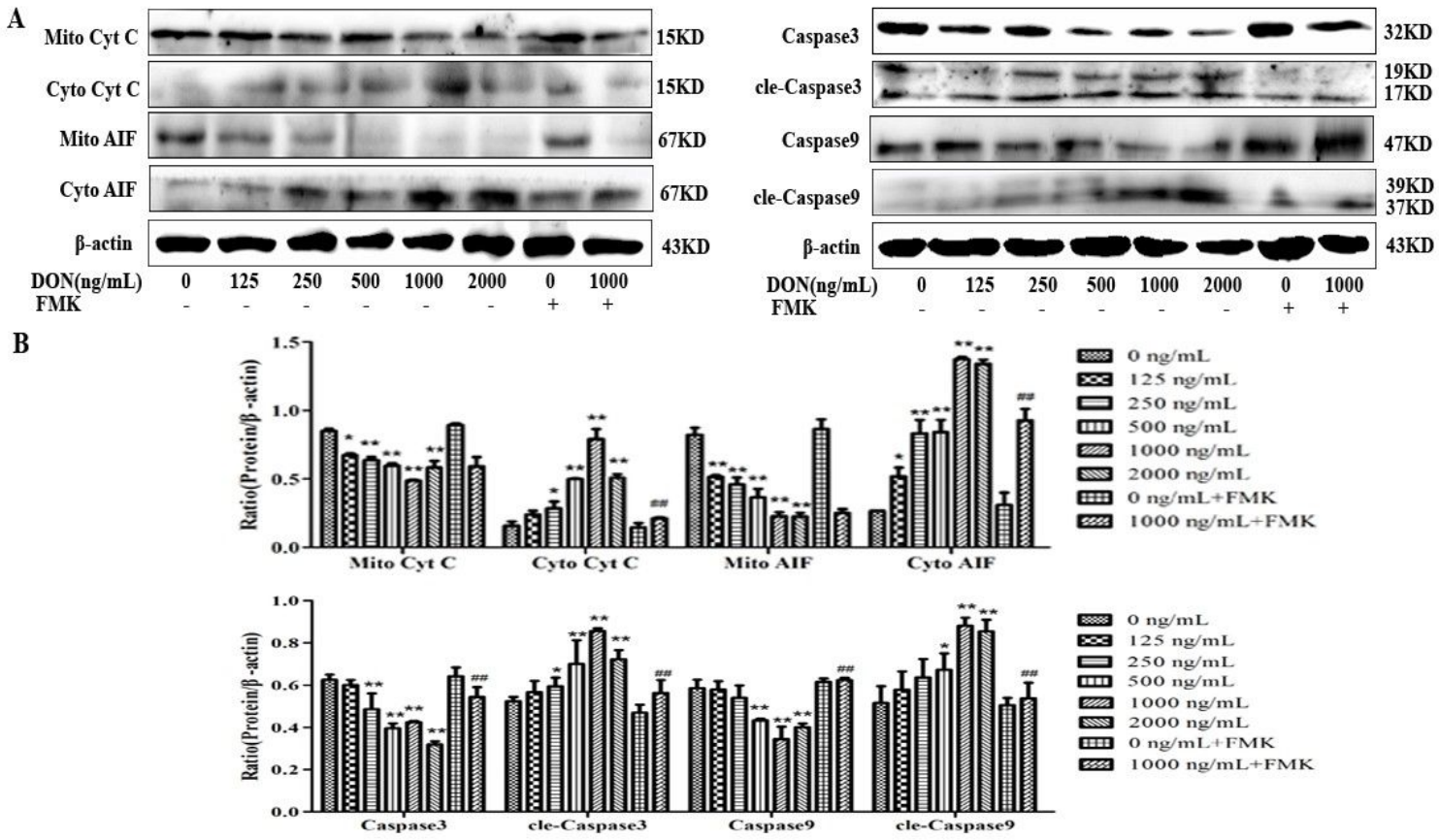

Figure 5

Effect of DON on apoptosis-related protein expression. A. Western blot was used to detect these proteins expression. B. The effect of DON on Caspase3, Caspase9,cleaved-Caspase9(cle-Caspase9), cleaved-Caspase3(cle-Caspase3), Cyt C and AIF expression. Date are mean values ± SD (n = 3). * Significant difference vs. controls (P< 0.05). ** Highly significant difference vs. controls (P< 0.01). ## Highly significant difference vs. 1000 ng/mL DON group (P< 0.01).

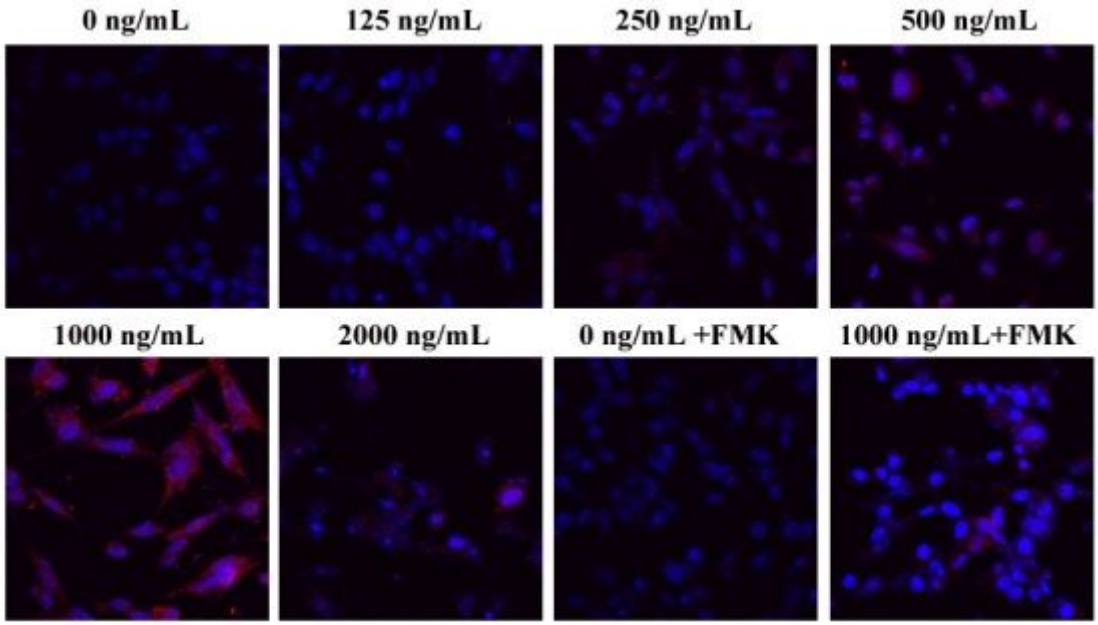

Figure 6

Effect of DON on Caspase3 activation. Cells were treated for 24 h with different concentrations of DON（0, 125, 250, 500, 1000, 2000 ng /mL, FMK, 1000 ng/mL DON+FMK) and cleaved-caspase-3 was then measured, subjected to immunofluorescence analysis of cleaved-caspase3 activation(red), and nuclei were counterstained with DAPI (blue).

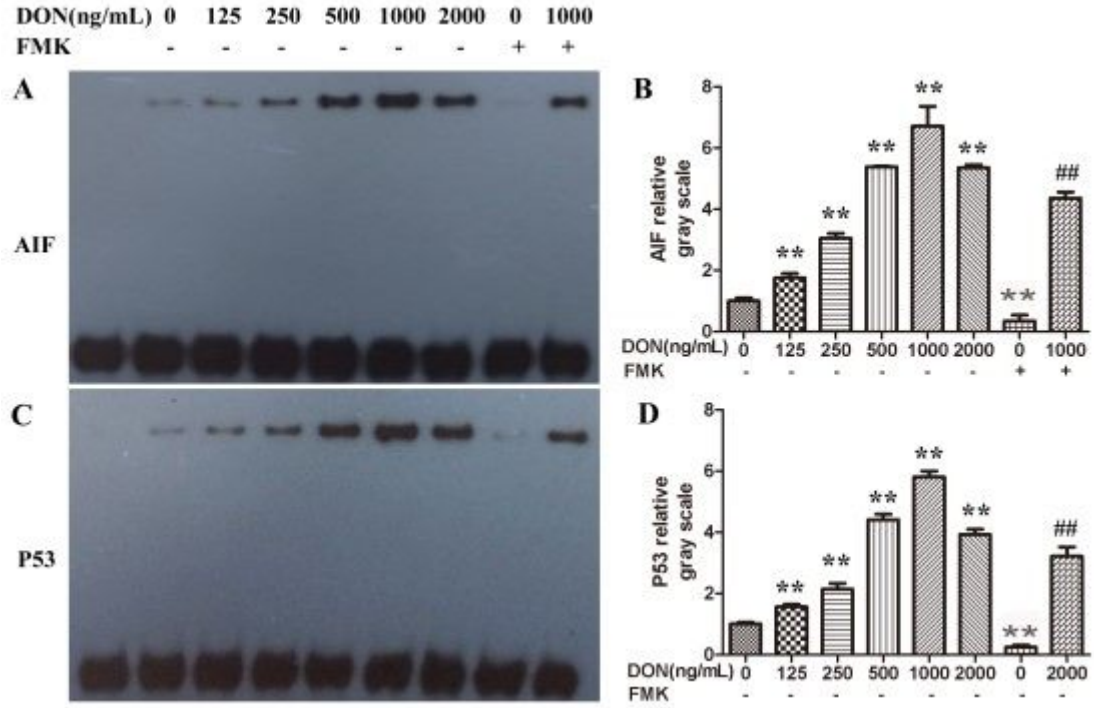

Figure 7

Effects of DON on the transcription activities of AIF and P53. Cells were treated for 24 h with different concentrations of DON（0, 125, 250, 500, 1000, 2000 ng /mL, FMK, 1000 ng/mL DON+FMK).Each treatment was replicated 3 times. Nuclear proteins were collected for the indicated time. (A) and (B) .The EMSA results of AIF; (C) and (D) The EMSA results of P53.Date are mean values ± SD (n = 3). ** Highly significant difference vs. controls (P< 0.01). ## Highly significant difference vs. 1000 ng/mL DON group (P< 0.01).

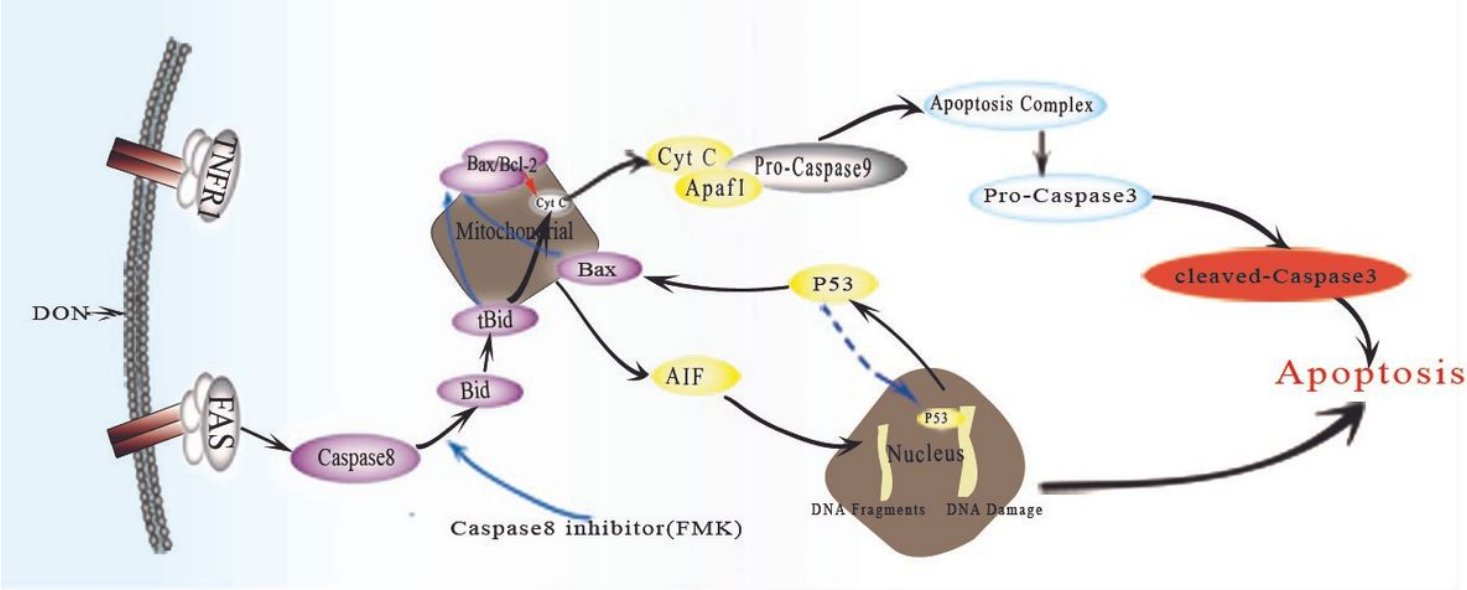

Figure 8

Illustrated schematic of study design and results.

Supplementary Files

This is a list of supplementary files associated with this preprint. Click to download.

- Highlights.doc
- GraphicalAbstract.tif